

# Fully-connected network of superconducting qubits in a cavity

Dimitris I. Tsomokos<sup>1,2</sup>, Sahel Ashhab<sup>2,3</sup>, Franco Nori<sup>2,3</sup>

<sup>1</sup>School of Physics, Astronomy & Mathematics, Science & Technology Research Institute, University of Hertfordshire, Hatfield AL10 9AB, UK

<sup>2</sup>Advanced Science Institute, Institute of Physical and Chemical Research (RIKEN), Wako-shi, Saitama 351-0198, Japan

<sup>3</sup>Center for Theoretical Physics, Physics Department, Applied Physics Program, Center for the Study of Complex Systems, The University of Michigan, Ann Arbor, Michigan 48109-1040, USA

E-mail: d.tsomokos@gmail.com, ashhab@riken.jp, fnori@riken.jp

**Abstract.** A fully-connected qubit network is considered, where every qubit interacts with every other one. When the interactions between the qubits are homogeneous, the system is a special case of the finite Lipkin-Meshkov-Glick model. We propose a natural implementation of this model using superconducting qubits in state-of-the-art circuit QED. The ground state, the low-lying energy spectrum and the dynamical evolution are investigated. We find that, under realistic conditions, highly entangled states of Greenberger-Horne-Zeilinger and W types can be generated. We also comment on the influence of disorder on the system and discuss the possibility of simulating complex quantum systems, such as Sherrington-Kirkpatrick spin glasses, with superconducting qubit networks.

PACS numbers: 03.67.-a, 75.10.Pq

## Introduction

The development of quantum information science has provided us with a fresh perspective on condensed-matter physics. In the last few years, new tools from quantum information theory have been applied to several problems in many-body physics [1]. At the center of this novel approach lies the problem of entanglement, that is, how to quantify the genuinely quantum correlations [2] in a many-body system and what these correlations can tell us about the system itself. The entanglement in a given system is also a resource for various quantum information processing tasks. Spin chains and lattices with short-range interactions have been studied extensively in this context. Although interactions between neighbors are more common, there are instances where long-range interactions give a better description of physical systems, such as certain types of spin glasses [3, 4]. It would be very interesting to be able to use quantum networks as simulators of such complex quantum systems. Furthermore, connected networks are attracting considerable interest in quantum information science [5] and in many other fields [6].

Here we study a fully-connected network, where every qubit interacts with every other one, irrespectively of the distances between them. Crucially, the proposed model is readily implementable with superconducting qubits [7]. The emerging field of circuit QED [7, 8, 9, 10] provides a natural system in which a large number of qubits can be coupled together. In such systems, superconducting qubits play the role of atoms, and a harmonic-oscillator circuit element plays the role of a cavity with which they interact. If a single ‘cavity’ is simultaneously coupled to a number of qubits, it will mediate coupling between all the possible qubit pairs [11]. If, in addition, the cavity is far off resonance with the qubits, its degrees of freedom can be integrated out of the problem and we obtain a system in which all the qubits are pairwise interacting. Previous studies have considered similar circuits for coupling arbitrarily distant superconducting qubits [12]. However, these studies relied on time-dependent pulses to selectively couple one qubit pair at a time, whereas here we consider the simultaneous coupling of all qubit pairs. An important incentive for studying the fully-connected network is that all the different elements for its construction are already in place in the laboratory.

Next we introduce the model, study its low-lying energy spectrum and its dynamical response, and discuss the influence of disorder. Our analysis mainly concerns the entanglement properties of small networks and the generation of highly-entangled states in near-future experiments with existing technologies of superconducting qubits in circuit QED. We also discuss the possibility of simulating spin glasses with these systems.

## Model and Hamiltonian

To begin with, we consider  $N$  charge (flux) qubits that are coupled capacitively (inductively) and assume that each qubit is operated at its degeneracy point [7].

Therefore the Hamiltonian is

$$\mathcal{H} = - \sum_{i=1}^N \frac{\Delta_i}{2} Z_i - \sum_{(i,j)} J_{ij} X_i X_j, \quad (1)$$

where the second sum runs over all possible qubit pairs. Here,  $\Delta_i > 0$  is the level splitting and  $J_{ij}$  is the strength of the coupling between qubits  $i$  and  $j$ .  $X_i$ ,  $Y_i$  and  $Z_i$  denote the Pauli matrices for qubit  $i$ . Multi-qubit entanglement generation has been analyzed in trapped ions and atoms using Hamiltonians of the form in Eq. (1) [13, 14]. In a circuit QED setup, which is the focus of this work, the macroscopic qubits allow individual addressing and readout, in addition to relatively straightforward scalability. Although additional terms will appear in the Hamiltonian of this system, these terms can be made negligibly small under realistic conditions, as was shown in Ref. [11].

If we let  $\Delta_i = \Delta$  and  $J_{ij} = J$  for all qubits, the system is homogeneous and it corresponds to a special case of the Lipkin-Meshkov-Glick model [1, 15]. In this case, the Hamiltonian can be expressed as

$$\mathcal{H} = -\frac{\Delta}{2} Z_{\text{Total}} - \frac{J}{2} X_{\text{Total}}^2 + \frac{NJ}{2}, \quad (2)$$

where  $Z_{\text{Total}} = \sum_{i=1}^N Z_i$  and  $X_{\text{Total}} = \sum_{i=1}^N X_i$ . From Eqs. (1) and (2) it is clear that the Hamiltonian commutes with the square of the total pseudo-spin operator,  $\sum_i (X_i + Y_i + Z_i)^2$ , and possesses spin-flip symmetry, i.e., it also commutes with  $\Pi_i Z_i$  [15].

## Ground state properties

Two parameter regimes can be identified, namely,  $\Delta \gg N|J|$  and  $\Delta \ll N|J|$ . In the first case, the single-qubit term in  $\mathcal{H}$  dominates and the preferred basis is the eigenbasis of  $Z$ ,  $\{|0\rangle, |1\rangle\}$ , with  $Z|0\rangle = |0\rangle$  (the eigenstates of  $X$  are denoted by  $\{|+\rangle, |-\rangle\}$ ). As  $|J| \rightarrow 0$  the ground state of the system becomes equal to the fully-separable state

$$|\Psi_{\text{SEP}}\rangle = |0\rangle^{\otimes N}. \quad (3)$$

We shall employ a pseudo-spin language for convenience; when  $J_{ij} < 0$  we say that the interaction is ‘antiferromagnetic’ (AFM), and when  $J_{ij} > 0$  we say that the interaction is ‘ferromagnetic’ (FM).

Secondly, if  $\Delta \ll N|J|$  then the interaction term in  $\mathcal{H}$  dominates and the preferred basis is the  $\{|+\rangle, |-\rangle\}$  basis. In this case the sign of  $J$  becomes important. For large, positive  $J$  (FM regime) the interaction term tends to set all the qubits in the same state in the  $\{|+\rangle, |-\rangle\}$  basis. The ‘ideal’ ground state of the system is approximately

$$|\Psi_{\text{GHZ}}\rangle = \frac{1}{\sqrt{2}} (|+\rangle^{\otimes N} + |-\rangle^{\otimes N}), \quad (4)$$

which is known as the GHZ-state [2]. In practice, however, this ideal state is typically fragile under small external perturbations. By contrast, for large and negative  $J$  (AFM regime) the interaction term favors a state in which pairs of neighbouring qubits are antiparallel in the  $\{|+\rangle, |-\rangle\}$  basis. Clearly, in a fully-connected geometry this condition

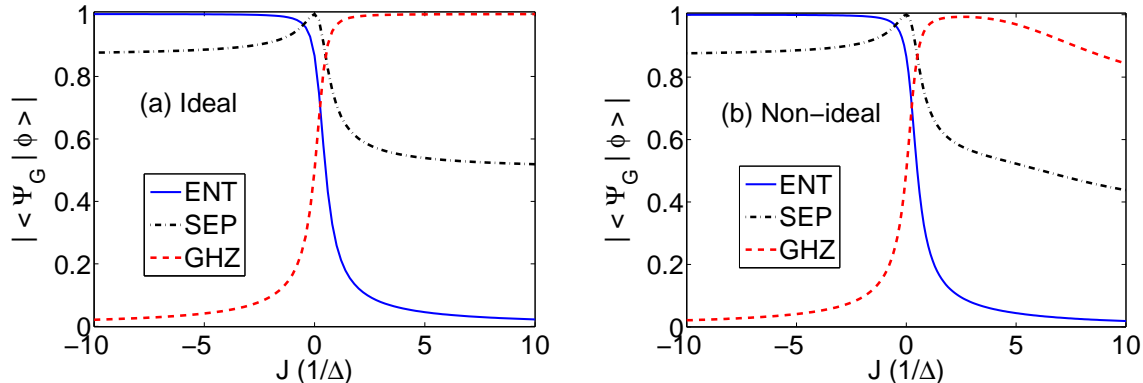


**Figure 1.** Fidelity  $|\langle \Psi_G | \phi \rangle|$  between the ground state,  $|\Psi_G\rangle$ , and the states  $|\Psi_{\text{SEP}}\rangle$ ,  $|\Psi_{\text{GHZ}}\rangle$ ,  $|\Psi_{\text{ENT}}\rangle$  against  $J$  for a network of  $N = 3$  qubits. We show (a) the ideal case and (b) the case where a small perturbation  $gX_i$  of strength  $g = \Delta/100$  is applied to qubit  $i$ .

is impossible to satisfy because every qubit neighbors every other qubit. This high degree of frustration in the system leads to highly-entangled states, as we show below. For the particular case of  $N = 3$  there is a relatively simple ground state, namely,

$$|\Psi_{\text{ENT}}\rangle = \frac{1}{\sqrt{3}} (|+ - 0\rangle + |- 0 +\rangle + |0 + -\rangle). \quad (5)$$

We illustrate the above statements by means of an exact numerical diagonalization,  $\mathcal{H}|\Psi_n\rangle = E_n|\Psi_n\rangle$  (for  $n = 1, 2, \dots$ ). In all numerical simulations, we let  $\Delta = 1$  and hence express the results in units of  $\Delta$ . In Fig. 1(a) we show the fidelity  $|\langle \Psi_G | \phi \rangle|$  between the ground state of the system,  $|\Psi_G\rangle$ , and the three states  $|\phi\rangle$  of Eqs. (3) to (5) for  $N = 3$ , in the ideal case. In Fig. 1(b) we calculate the same fidelities but now we apply a small perturbation  $gX_i$ , of strength  $g \ll \Delta$ , to qubit  $i$  (it does not matter which one). The symmetry-breaking term only affects the FM regime, where the  $|\Psi_{\text{GHZ}}\rangle$  becomes increasingly fragile as  $J$  is increased beyond a certain optimal value. This result holds for all small networks with  $N \sim 10$ : it is always possible to find an optimal value of the coupling strength such that the ground state is very close to a GHZ-state, even in the presence of a small external perturbation. For larger networks, or stronger perturbations, the behaviour is more abrupt and we do not obtain exact or almost exact GHZ-states, in practice.

In Fig. 2(a) the full energy spectrum for the  $N = 3$  case is presented. In Fig. 2(b) the lower half of the spectrum for  $N = 4$  is presented. One can see that the ground state is unique in the AFM regime and two-fold degenerate in the FM regime. Also, there is a finite energy gap between the ground states and the first excited states, which remains constant with increasing  $|J|$  in the AFM regime and increases with  $|J|$  in the FM regime.

We now turn to the entanglement properties of the different possible ground states. We consider both the entanglement between pairs of qubits and also between blocks of qubits. Among the various measures of two-qubit entanglement [2], we calculate the

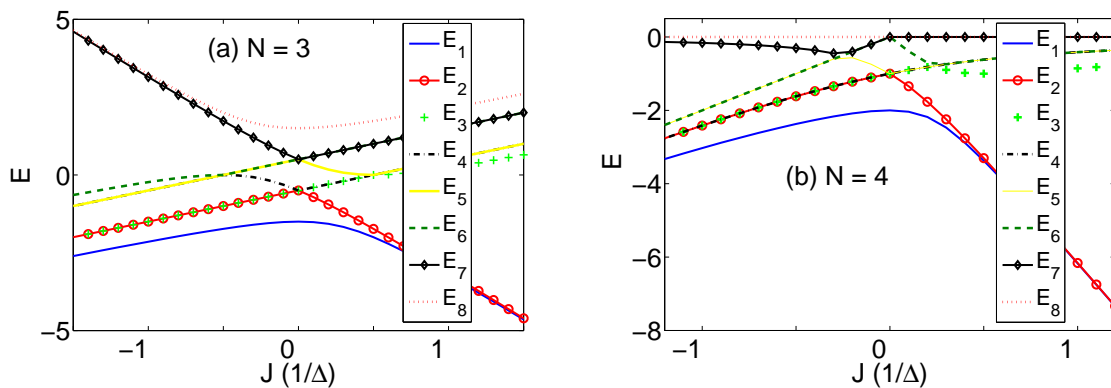


**Figure 2.** (a) Full energy spectrum for a system of size  $N = 3$  against  $J$ . (b) Lower half of the energy spectrum, versus  $J$ , for a system of size  $N = 4$ .

logarithmic negativity [16]. It is defined as

$$E_N(\rho_{ij}) \equiv \log_2 \|\rho_{ij}^{T_i}\|, \quad (6)$$

where  $\|\cdot\|$  denotes the trace norm of a matrix and  $\rho_{ij}^{T_i}$  is the partial transpose of the reduced density matrix  $\rho_{ij}$  of two qubits  $i$  and  $j$ . We also use the von Neumann entropy of a state  $\rho_k$ , for a block of  $k < N$  qubits,

$$S(\rho_k) \equiv -\text{tr}(\rho_k \log_2 \rho_k). \quad (7)$$

$S(\rho_k)$  quantifies how mixed is the reduced density matrix  $\rho_k$  and, if the system as a whole is in a pure state, it also quantifies the amount of entanglement between the qubits in the set  $k$  and those in the rest of the system.

The pairwise entanglement,  $E_N(\rho_{ij})$ , is shown in Fig. 3(a) against  $J$  for systems of size  $N = 3, 4, \dots, 12$ . We observe that  $E_N(\rho_{ij})$  decreases with the size of the system  $N$ . This can be explained by the fact that as  $N$  increases so do the number of interactions for each individual qubit. This higher degree of connectivity places stronger monogamy constraints that generally reduce the two-party entanglements [17]. To study the many-body correlations of the ground state, we show in Fig. 3(b) the entanglement of a single qubit  $i$  with the rest of the system, using the von Neumann entropy  $S(\rho_i)$ . In the FM regime the ideal ground state is a GHZ state, in which every qubit is maximally entangled with the rest of the network. In practice, however, under the influence of an external perturbation, the system chooses one of the two degenerate eigenstates and becomes fully separable in the deep FM regime. This is seen in the inset of Fig. 3(b), which shows the ground state of a small network perturbed by  $gX_i$  with strength  $g = \Delta/100$ . In the AFM regime,  $S(\rho_i)$  increases with the size of the network for odd  $N$  and it decreases for even  $N$ . This is due to the different symmetries in the two cases, which appear for small networks but disappear in the thermodynamic limit (see, e.g., [15]). In summary, in the AFM regime the system achieves multi-qubit entanglement for any  $|J| > 0$ ; in the FM regime the system achieves a high degree of multi-qubit entanglement in practice, approaching a GHZ-state, for an optimal value of the interaction strength, while deep in the FM regime it becomes fully separable.

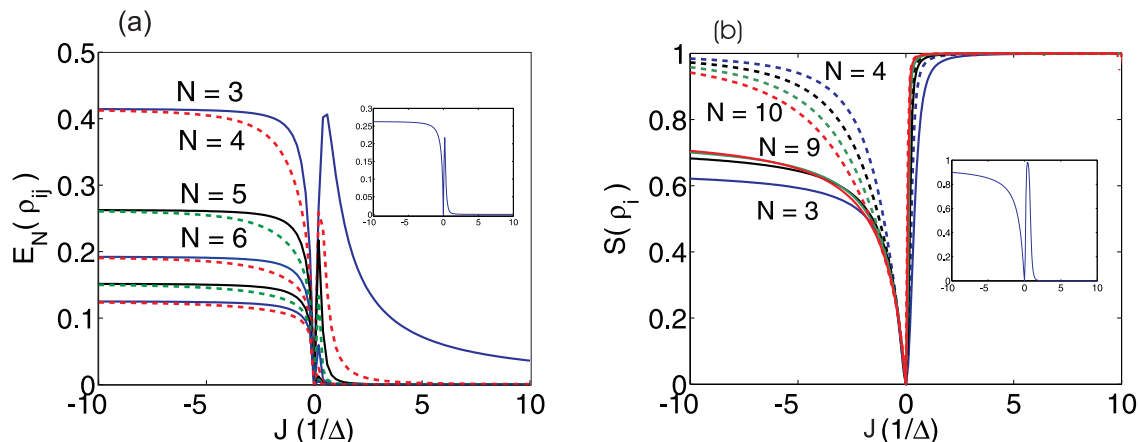


**Figure 3.** (a)  $E_N(\rho_{ij})$  against  $J$  for networks of size  $N = 3$  to  $N = 12$  (from top to bottom). (b)  $S(\rho_i)$  against  $J$  for  $N = 3$  to  $N = 10$ . Solid lines correspond to  $N = 3, 5, 7, 9$  (from bottom to top) and broken lines to  $N = 4, 6, 8, 10$  (from top to bottom), as indicated. In both (a) and (b), the insets correspond to the  $N = 5$  case with a small perturbation  $gX_i$  of strength  $g = \Delta/100$ .

## Dynamical evolution

Next, we study the system's evolution, which is determined by the state

$$|\Psi(t)\rangle = \exp(-i\mathcal{H}t)|\Psi(0)\rangle. \quad (8)$$

We consider two simple initial states: the state  $|\Psi_{\text{SEP}}\rangle$  of Eq. (3), and the state  $|\Psi_{\text{SEP}}^{(1)}\rangle = |1\rangle \otimes |0\rangle^{\otimes N-1}$ , which is the same as  $|\Psi_{\text{SEP}}\rangle$  except that the state of one qubit is flipped. Both of these states are separable and easy to prepare experimentally. For definiteness we assume that  $J > 0$ , and we only consider the case of weak coupling, which is most relevant to near-future experiments.

In the weak-coupling limit,  $J \ll \Delta/N$ , one can classify the low-lying states according to the number of elementary excitations they contain. The ground state  $|\Psi_{\text{SEP}}\rangle$  contains no excitations and does not evolve in time. At an energy  $\sim \Delta$  above the ground state, there are  $N$  energy eigenstates that can be identified as one-excitation states. These states have the ‘spin-wave’ form  $|\Phi_{1,k}\rangle = \frac{1}{\sqrt{N}} \sum_{j=1}^N e^{2\pi ijk/N} |0_1 \cdots 0_{j-1} 1_j 0_{j+1} \cdots 0_N\rangle$ , where  $k = 0, 1, \dots, N-1$ . Their energies (relative to the ground state) are given by  $\Delta - (N-1)J$  for  $k = 0$  and  $\Delta + J$  otherwise. As these  $N$  energy eigenstates are separated from all other states by an energy at least  $\sim \Delta$ , their dynamics can be analyzed in the restricted Hilbert space containing only these  $N$  states. Using the above spectrum, we find that the initial state  $|\Psi(t=0)\rangle = |\Psi_{\text{SEP}}^{(1)}\rangle$  evolves, up to an overall phase factor, into

$$|\Psi(t)\rangle = |\Psi_{\text{SEP}}^{(1)}\rangle + \frac{\exp(iNJt) - 1}{\sqrt{N}} |W_N\rangle, \quad (9)$$

where the ‘W-state’ [2] is  $|W_N\rangle = \frac{1}{\sqrt{N}} \sum_{j=1}^N |0_1 \cdots 0_{j-1} 1_j 0_{j+1} \cdots 0_N\rangle$ . From this result we observe that the evolved state is a time-dependent superposition of  $|\Psi_{\text{SEP}}^{(1)}\rangle$  and  $|W_N\rangle$ .

For large networks ( $N \rightarrow \infty$ ) the second term can be neglected, and the system remains close to its initial state (the initial excitation is localized). For  $N = 3$  and  $N = 4$ , on the other hand, Eq. (9) reduces to variants of the W-state (when  $|e^{iN Jt} - 1| = \sqrt{N}$ ),

$$\begin{aligned} |\mathcal{W}_3\rangle &= \frac{e^{\pm i\pi/6}}{\sqrt{3}}|100\rangle + \frac{e^{\pm 5i\pi/6}}{\sqrt{3}}(|010\rangle + |001\rangle) \\ |\mathcal{W}_4\rangle &= \frac{1}{2}(-|1000\rangle + |0100\rangle + |0010\rangle + |0001\rangle). \end{aligned} \quad (10)$$

For larger, but still weak, coupling we study the evolution using the fidelity between  $|\Psi(t)\rangle$  and the GHZ and W states. If the initial state is  $|\Psi_{\text{SEP}}\rangle$ , then the system evolves into a state that is close to a GHZ-state; if the initial state is  $|\Psi_{\text{SEP}}^{(1)}\rangle$ , then the system evolves into a state that is close to a W-state, for small networks. For  $N = 3$  and  $N = 4$ ,  $|\Psi(t)\rangle$  can be made arbitrarily close to  $|\Psi_{\text{GHZ}}\rangle$  or  $|\mathcal{W}\rangle$  for properly chosen values of  $J$  (see Fig. 4). It is possible to achieve multi-qubit entanglement of these two types with networks of size  $N > 4$ , but the window for the required coupling strengths is much sharper and the fidelity maxima decrease below 1. For instance, for  $N = 6$  and  $0 < J < \Delta/2$  the maximum fidelity of the evolved state with the GHZ-state is 0.96, which is still a relatively high fidelity [18].

Thus, the fully connected network is well suited for the fast (one-step) preparation of GHZ- and W- entangled states. This result should be contrasted with recent work on the generation of entangled states in superconducting qubit circuits using generally long sequences of basic operations [19]. For networks with  $N > 4$  and the simple initial states used above, we obtain entangled states that are different from the GHZ- and W-states, but still highly entangled and therefore of potential value for future quantum information technologies (e.g., we only mention applications related to quantum secret sharing and quantum average estimation [20]).

Finally, we note that the dynamics of entanglement has simple periodicity only in the case of  $N = 3$ , which corresponds to a closed chain. In general, for  $N > 3$ , the behavior of the logarithmic negativity  $E_N(\rho_{ij})$  is complicated and there are time intervals for which it drops to zero. As the system size increases, so does the durations of these time intervals. During most of the intervals in which the pairwise entanglements vanish, the block entanglements increase to their local maxima. Therefore the system achieves a form of multi-qubit entanglement. On the other hand, for small and negative  $J$  we find that the evolution of entanglement shows more periodic features. The block entropies  $S(\rho_k)$  (for different block sizes  $k$ ) have their local maxima at the same times as the  $E_N(\rho_{ij})$ . Hence in the AFM regime the system evolves into an entangled state that is different from the GHZ- and W-states.

## Static disorder

In the presence of disorder, a system with the Hamiltonian  $\mathcal{H}(\Delta_i, J_{ij})$  of Eq. (1) is inhomogeneous. As a result, different partitions of the network that correspond to the same number of qubits are no longer equivalent. We study the influence of uniform,



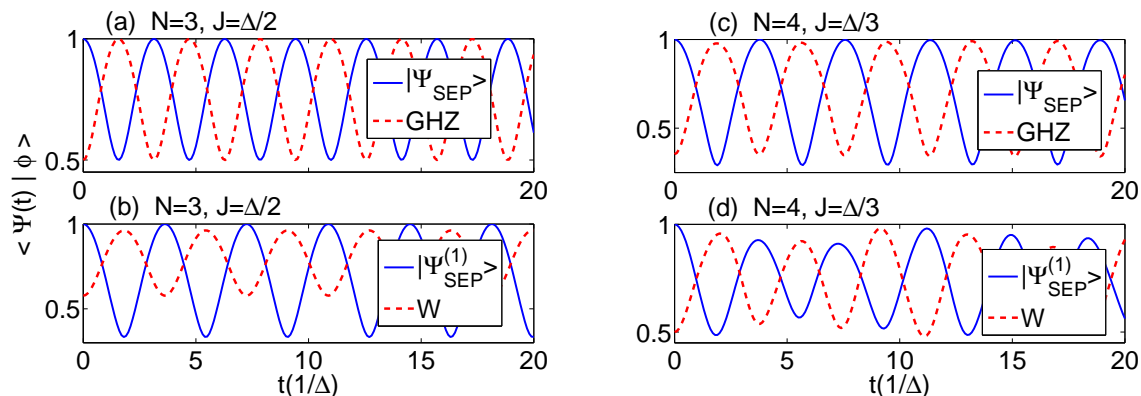


**Figure 4.** Fidelity  $|\langle \Psi(t) | \phi \rangle|$  between the evolved state and the different initial states, the GHZ-state of Eq. (4) and the W-state of Eq. (10), as indicated. (a) and (b) correspond to  $N = 3$ ,  $J = \Delta/2$ , while (c) and (d) correspond to  $N = 4$ ,  $J = \Delta/3$ .

static disorder on the system by assuming that the  $J_{ij}$  and the  $\Delta_i$  are chosen randomly from the intervals  $[1 - \delta_1, 1 + \delta_1]J$  and  $[1 - \delta_2, 1 + \delta_2]\Delta$ , respectively, where  $\delta_{1,2} \in [0, 1]$  quantify the amount of disorder in each parameter. We neglect the type of disorder that can move a qubit away from its degeneracy point, but this is a valid approximation for realistic implementations. The properties of the low-lying energy sector and the dynamics are studied as an average over many realizations of  $\mathcal{H}(\Delta_i, J_{ij})$ . We only consider the weak-coupling regime, and the case of small networks.

We shall not show any details on these Monte-Carlo simulations, as they do not add any insight beyond the main conclusions. From the numerical calculations, we observe that disorder in the  $J_{ij}$  is more important than disorder in the  $\Delta_i$ . More crucially, we find that the results reported here, including those on the ground state entanglement and the dynamics of entanglement, remain largely unaffected for disorder of amount  $\delta_{1,2} \leq 10\%$ . This result is in agreement with previous studies on disorder [21], and it is an experimentally achievable upper bound.

## Spin glasses

The simplest examples of glassy systems are spin glasses and they offer the possibility of studying the behavior of complex systems away from equilibrium. Spin glasses arise when the interactions between spins are ferromagnetic for some bonds and antiferromagnetic for others, in which case the spin orientation cannot be uniform in space even at low temperatures [3]. In this case the spin orientation can become random and frozen in time. A particularly illuminating and extensively studied model of spin glasses is the Sherrington-Kirkpatrick (SK) model. The SK model in a transverse field [4] is given by the Hamiltonian  $\mathcal{H}$  of Eq. (1) for interactions that are disordered in both magnitude and sign. In fact, if the distribution of  $J_{ij}$  is Gaussian, then for  $J \sim \Delta$  the system is a spin glass for temperatures lower than  $k_B T \sim \Delta/4$  (see, e.g., [4]).

There are various important open problems in this field, both theoretical and



experimental. For instance, in relation to the proposal of the present work, one such problem is the behavior of spin glasses in the low temperature phase region, where quantum phenomena dominate (see, e.g., Parisi in [3]). Some of the advantages of using qubit networks as quantum simulators include the fact that the states of all the qubits can be prepared controllably and that the dynamics of all the qubits can be monitored as a function of time, yielding the ‘microscopic’ dynamics of individual spins and not just averaged spin quantities. Therefore the implementation of fully-connected networks with superconducting qubits, which can be addressed and measured individually, can offer valuable additional tools for the study of complex quantum systems, such as spin glasses.

## Outlook and summary

In this work we have focused on  $XX$ -type interqubit couplings [Eq. (1)] since this is relevant to present-day experiments in circuit QED. A modified version of the flux qubit was proposed recently, which implements  $ZZ$ -type couplings [22]. This form of the coupling could give rise to other types of many-body entangled quantum states [23]. We have also focused on the case where the cavity is far off resonance with the qubits. Bringing the cavity into resonance with the qubits would lead to a star geometry with the cavity at the center of the star. In this case, the Hamiltonian of Eq. (1) is no longer valid; instead, each qubit interacts only with the cavity and not other qubits. The addition of a nonlinearity to the cavity can be used to make the center of the star an effective two-level system [24].

In conclusion, we have proposed an implementation of a qubit network where all qubits are coupled in pairs, independently of the relative distances between them, as in the finite LMG model of spin systems. Such a network supports a highly-entangled ground state in the case of antiferromagnetic interactions, which is robust against small external perturbations. Under suitable conditions, separable initial states evolve into exact GHZ- and W-type states in the case of small networks, or other highly-entangled states for larger networks. The qualitative behavior of the system is unaffected by the presence of static disorder, as long as the amount of disorder is under about 10%. Thus the system is well-suited for the generation of many-body entangled states with macroscopic superconducting qubits. The presence of entanglement in such systems can be witnessed experimentally via combinations of two-qubit correlation measurements, as for example described in Ref. [21]. Another promising prospect is the simulation of spin glasses. The fully-connected network could be realized experimentally in the near future with superconducting qubits in circuit QED.

## Acknowledgments

We would like to thank A. Galiatdinov for useful discussions. This work was supported in part by the NSA, LPS, ARO, NSF (grant No. EIA-0130383) and the JSPS-CTC

program. DIT acknowledges the support of the EPSRC (EP/D065305/1).

## References

- [1] L. Amico, R. Fazio, A. Osterloh, V. Vedral, *Rev. Mod. Phys.* **80**, 517 (2008).
- [2] R. Horodecki, P. Horodecki, M. Horodecki, K. Horodecki, arXiv:quant-ph/0702225 (2007); M.B. Plenio and S. Virmani, *Quant. Inf. Comp.* **7**, 1 (2007).
- [3] K. Binder and A.P. Young, *Rev. Mod. Phys.* **58**, 801 (1986); H. Nishimori, *Statistical Physics of Spin Glasses and Information Processing* (Oxford University Press, 2001); G. Parisi, *Proc. Natl. Acad. Sci.* **103**, 7948 (2006).
- [4] D. Thirumalai, Q. Li, T.R. Kirkpatrick, *J. Phys. A* **22**, 3339 (1989); M.J. Rozenberg and L. Arrachea, *Physica B* **312**, 416 (2002).
- [5] A. Acín, J.I. Cirac, M. Lewenstein, *Nature Physics* **3**, 256 (2007).
- [6] R. Albert and A.-L. Barabási, *Rev. Mod. Phys.* **74**, 47 (2002); M. Newman, A.-L. Barabási, D.J. Watts, *The Structure and Dynamics of Networks* (Princeton University Press, 2006).
- [7] J.Q. You and F. Nori, *Phys. Today* **58** (11), 42 (2005); J. Clarke and F.K. Wilhelm, *Nature* **453**, 1031 (2008).
- [8] I. Chiorescu, P. Bertet, K. Semba, Y. Nakamura, C.J.P.M. Harmans, J.E. Mooij, *Nature* **431**, 159 (2004).
- [9] A. Wallraff, D.I. Schuster, A. Blais, L. Frunzio, R.-S. Huang, J. Majer, S. Kumar, S.M. Girvin, R.J. Schoelkopf, *Nature* **431**, 162 (2004).
- [10] J. Johansson, S. Saito, T. Meno, H. Nakano, M. Ueda, K. Semba, H. Takayanagi, *Phys. Rev. Lett.* **96**, 127006 (2006).
- [11] See e.g., S. Ashhab, A.O. Niskanen, K. Harrabi, Y. Nakamura, T. Picot, P.C. de Groot, C.J.P.M. Harmans, J.E. Mooij, F. Nori, *Phys. Rev. B* **77**, 014510 (2008). The derivation of the mediated-coupling Hamiltonian in the multi-qubit case follows closely that of the two-qubit case.
- [12] See e.g., Y. Makhlin, G. Schön, A. Shnirman, *Rev. Mod. Phys.* **73**, 357 (2001); J. Q. You, J. S. Tsai, and F. Nori, *Phys. Rev. Lett.* **89**, 197902 (2002).
- [13] K. Molmer and A. Sorensen, *Phys. Rev. Lett.* **82**, 1835 (1999); K. Helmeron and L. You, *ibid.* **87**, 170402 (2001); S.-B. Zheng, *ibid.* **87**, 230404 (2001).
- [14] Multipartite entangled states were also studied in the related system of a Bose-Einstein condensate whose constituent atoms possess an internal spin (or pseudospin) degree of freedom; C. K. Law, H. Pu, and N. P. Bigelow, *Phys. Rev. Lett.* **81**, 5257 (1998); T.-L. Ho and S.-K. Yip, *Phys. Rev. Lett.* **84**, 4031 (2000); A. B. Kuklov and B. V. Svistunov, *Phys. Rev. Lett.* **89**, 170403 (2002); S. Ashhab and A. J. Leggett, *Phys. Rev. A* **68**, 063612 (2003).
- [15] H.J. Lipkin, N. Meshkov, A. J. Glick, *Nucl. Phys.* **62**, 188 (1965); J. Vidal, G. Palacios, Cl. Aslangul, *Phys. Rev. A* **70**, 062304 (2004); S. Dusuel and J. Vidal, *Phys. Rev. Lett.* **93**, 237204 (2004); T. Barthel, S. Dusuel, J. Vidal, *Phys. Rev. Lett.* **97**, 220402 (2006); P. Ribeiro, J. Vidal, R. Mosseri, *Phys. Rev. E* **78**, 021106 (2008); R. Ors, S. Dusuel, J. Vidal, *Phys. Rev. Lett.* **101**, 025701 (2008).
- [16] M.B. Plenio, *Phys. Rev. Lett.* **95**, 090503 (2005).
- [17] V. Coffman, J. Kundu, W.K. Wootters, *Phys. Rev. A* **61**, 052306 (2000); A. Ferraro, A. García-Saez, A. Acín *Phys. Rev. A* **76**, 052321 (2007).
- [18] Recently it was shown that, in the weak-coupling limit and by applying appropriate single-qubit rotations at appropriate times, GHZ states with fidelity 1 can be prepared for an arbitrary number of qubits in this system (with a preparation time that is independent of the number of qubits); A. Galiatdinov, unpublished [see also A. Galiatdinov and J.M. Martinis, *Phys. Rev. A* **78**, 010305 (2008)]. It can be expected that the application of the proper single-qubit rotations will result in high-fidelity preparation of W states as well.
- [19] C.-P. Yang and S. Han, *Phys. Rev. A* **70**, 062323 (2004); L. F. Wei, Y.-x. Lui, F. Nori, *Phys. Rev. Lett.* **96**, 246803 (2006); R. Migliore, K. Yuasa, H. Nakazato, and A. Messina, *Phys. Rev. B* **74**,

- 104503 (2006); S. Matsuo, S. Ashhab, T. Fujii, F. Nori, K. Nagai, and N. Hatakenaka, *J. Phys. Soc. Jpn.* **76**, 054802 (2007).
- [20] M. Hillery, V. Buzek, A. Berthiaume, *Phys. Rev. A* **59**, 1829 (1999); C. Schmid, P. Trojek, H. Weinfurter, M. Bourennane, M. Zukowski, C. Kurtsiefer, *Phys. Rev. Lett.* **95**, 230505 (2005); A.M. Wang, *Phys. Rev. A* **75**, 062323 (2007); C. Di Franco, M. Paternostro, M.S. Kim, *Phys. Rev. A* **77**, 020303(R) (2008); C. Di Franco, M. Paternostro, D.I. Tsomokos, S.F. Huelga, *Phys. Rev. A* **77**, 062337 (2008) and references therein.
- [21] D.I. Tsomokos, M.J. Hartmann, S.F. Huelga, M.B. Plenio, *New J. Phys.* **9**, 79 (2007).
- [22] A.J. Kerman and W.D. Oliver, *Phys. Rev. Lett.* **101**, 070501 (2008).
- [23] M. Hein, W. Dür, J. Eisert, R. Raussendorf, M. Van den Nest, H.-J. Briegel, arXiv:quant-ph/0602096 (2006); W. Dür, L. Hartmann, M. Hein, M. Lewenstein, H.-J. Briegel, *Phys. Rev. Lett.* **94**, 097203 (2005).
- [24] A. Hutton and S. Bose, *Phys. Rev. A* **69**, 042312 (2004).